Fuel savings on missed approach through aircraft reinjection

María Carmona, Rafael Casado González and Aurelio Bermúdez
Albacete Research Institute of Informatics, Universidad de Castilla-La Mancha – Campus de Albacete, Albacete, Spain
Miguel Pérez-Francisco
Computer Science and Engineering Department, Universitat Jaume I, Castellón, Spain
Pablo Boronat
Computer Languages and Systems Department, Universitat Jaume I, Castellón, Spain, and
Carlos Calafate
Department of Computer Engineering, Universitat Politècnica de València, Valencia, Spain

Abstract

Purpose – In the aerial transportation area, fuel costs are critical to the economic viability of companies, and so urgent measures should be adopted to avoid any unnecessary increase in operational costs. In particular, this paper addresses the case of missed approach manouevres, showing that it is still possible to optimize the usual procedure.

Design/methodology/approach – The costs involved in a standard procedure following a missed approach are analysed through a simulation model, and they are compared with the improvements achieved with a fast reinjection scheme proposed in a prior work.

Findings – Experimental results show that, for a standard A320 aircraft, fuel savings ranging from 55% to 90% can be achieved through the reinjection method.

Originality/value – To the best of the authors' knowledge, this work is the first study in the literature addressing the fuel savings benefits obtained by applying a reinjection technique for missed approach manoeuvres.

Keywords Air traffic management, Missed approach, Base of Aircraft Data, Fuel consumption, Environmental impact

Paper type Research paper

Nomenclature

Symbols

D = aerodynamic drag force (N);
C_D = drag coefficient;
C_{D_0} = parasitic drag coefficient;
C_{D_2} = induced drag coefficient;
C_{f1} = 1st fuel coefficient ($kg/(min \times kN)$);
C_{f2} = 2nd trust specific fuel consumption coefficient (kt);
C_{f3} = 3rd trust specific fuel consumption coefficient (kg/min);
C_{f4} = 4th trust specific fuel consumption coefficient (ft);
γ = path angle (rad);
ρ = local air density (kg/m^3);
C_L = lift coefficient;
F = fuel flow (kg/min);
g = gravitational acceleration (m/s^2);
h = geodetic altitude (m);
L = aerodynamic lift force (N);
m = aircraft mass (kg);
S = reference wing surface area (m^2);
T = engine thrust force (N);
V = true airspeed (m/s);
W = aircraft weight (N);
η = trust specific fuel flow ($kg/(min \times kN)$);
T_s = aircraft spacing (s);
T_1 = threshold time (for gap search) (s);
T_{air} = air temperature (K);
p = air pressure (Pa); and
R = air constant ($m^2/K\,s^2$).

The current issue and full text archive of this journal is available on Emerald Insight at: **https://www.emerald.com/insight/1748-8842.htm**

Aircraft Engineering and Aerospace Technology
96/2 (2024) 248–256
Emerald Publishing Limited [ISSN 1748-8842]
[DOI 10.1108/AEAT-11-2022-0305]

This work is derived from R&D projects RTI2018-098156-B-C52 and RTI2018-096384-B-I00, funded by MCIN/AEI/10.13039/501100011033 and "ERDF A way of making Europe", by the Junta de Comunidades de Castilla-La Mancha under grant SBPLY/19/180501/000159, and by the Universidad de Castilla–La Mancha under grant 2021-GRIN-31042.

Received 17 November 2022
Revised 24 October 2023
Accepted 9 November 2023

Introduction

Conventional aircraft emit not only different pollutants such as carbon, nitrogen or sulphur oxides, but also unburnt fuel and other particulates. In particular, CO_2 emissions are usually taken as a reference metric to determine the overheads associated to different phases of the flight, pinpointing which phases have more margin for improvement.

As early as 2006, Lu and Morrell (2006) proposed a pollution and noise model for airports from an economical perspective, as the intention of many countries is to restrict the pollution regulations. This model is focused on landing and take-off operations. In addition, in European Union Aviation Safety Agency (EASA, 2019), it is highlighted that, despite all traffic management operations already benefit from highly optimized procedures, there is still room for improvement, especially for the take-off and landing processes. It is well known that one of the procedures with margin for optimization in large airports is the handling of missed approaches.

The conventional missed approach procedure consists of restarting the manoeuvre from the beginning. In Casado *et al.* (2021), an alternative procedure, known as Aircraft Reinjection System (ARS), is proposed and evaluated. The method basically consists in redirecting the affected aircraft towards an existing gap in the approach flow. ARS detects the existence of that gap, estimates its future position and determines a new set of waypoints that define a route to quickly reinject the aircraft in the flow. These waypoints are provided to the aircrew by the air traffic controllers. As a result, the aircraft is fully integrated as standard traffic on the approach flow. At the same time, the new route maintains safety separation standards [International Civil Aviation Organization (ICAO), 2016].

In this paper a deep analysis is presented about how ARS can benefit both the air company and the environment by reducing the amount of fuel spent in the case of missed approaches. To estimate fuel consumption, the Base of Aircraft Data (BADA) model is used [European Organisation for the Safety of Air Navigation (Eurocontrol), 2023; Nuic *et al.*, 2010]. The accuracy of this model has been validated by several studies (HARADA *et al.*, 2013; Poles *et al.*, 2010). Experiments performed using our landing simulation tool show that, on a standard A320 aircraft, fuel savings ranging from 55% to 90% are feasible.

A few previous works addressed fuel consumption and pollutant emissions during missed approach manoeuvres. First, according to Boeing (2007), the fuel burned during a missed approach is equivalent to 2 to 28 times the fuel burn required for a descent and approach. This publication details the additional amount of fuel burned by different Boeing aircraft models.

In Dancila *et al.* (2013) the authors used data published by the European Environment Agency (EEA) [European Environment Agency (EEA), 2023] to estimate fuel burn and emissions for a B737-400 aircraft performing a missed approach procedure in one of the runways of Seattle's Airport. Compared to a reference standard approach, a missed approach burns 2.84 times more fuel without a holding pattern and 3.53 times more for a 20 NM holding pattern.

On the other hand, the authors of Murrieta-Mendoza and Botez (2016) proposed a method to estimate the fuel burnt, and the pollution generated by a successful landing and by a missed approach procedure followed by a successful landing. As in the previous work, computations are based on the EEA database.

Our work differs from the previous ones (besides fuel consumption estimation being based on the BADA model) in that we specifically focus on the fuel savings achievable when adopting the ARS method, and analysis that has not been done by any other authors in the past.

The remainder of this paper is structured as follows. In the next section we describe the conventional missed approach procedure and present an overview of the ARS solution. Then, *BADA3 Model* section details the model that provides the performance (including fuel consumption) of an aircraft during take-off and landing when following standard procedures. Afterward, *methodology* section details our simulator and the configuration for the chosen scenario to conduct the simulations. Subsequently, there is a section dedicated to *simulation results*, which is followed by *discussion* section. Finally, the main conclusions and future works are drawn in sections *conclusions* and *future work*, respectively.

Improving the missed approach procedure

In standard instrument approach procedures (IAP) (Federal Aviation Administration (FAA), 2023a) pilots are supported by several navigation aids, such as the Instrument Landing System (Moir *et al.*, 2013), and follow an instrument approach chart that contains all the necessary information. An IAP comprises several segments, referred to as initial, intermediate and final segments, and may also include a missed approach segment. Each approach segment is defined by a pair of starting and ending fixes, which correspond with geographical positions. These fixes are the initial approach fix (IAF), the intermediate fix (IF) and the final approach point (FAP).

To illustrate this procedure, the path to be followed by an aircraft approaching to runway RWY 13 at Málaga airport (International Civil Aviation Organization (ICAO), 2023) is represented by a blue line in Figure 1 (either a or b). In Figure 1, latitude and longitude are expressed in metres with respect to a reference system centred at the runway touchdown point, the runway being represented by a green line. We assume that aircraft enter the airport airspace through the LOJAS waypoint and then fly to TOLSU, which is the IAF. After that, they proceed to MARTIN, where they turn left and progressively descend, first to the IF (MG402) and then to the FAP (MG401). From there, they cover the final approach segment to the runway (RWY13).

A missed approach procedure is the procedure to be followed by the aircraft if, due to any circumstance, an approach to land cannot be safely executed [Federal Aviation Administration (FAA), 2023b]. Once the pilot makes the decision of aborting the landing, he/she is expected to notify it by radio to the air traffic control service (ATC) as soon as possible. Then, once the missed approach point (MAPt) defined on the chart has been reached, the pilot must follow the instructions indicated or an alternative manoeuvre provided by the ATC. Current missed approach procedures are based on traditional radio aids-based navigation. Charts usually propose a pattern that, in a best-case scenario, reroutes the aircraft to the IAF.

In the case of Málaga airport, the chart establishes that the aircraft must maintain the same heading as that of the runway for about 20 NM and then join the XILVI point. Once there, the aircrew must await ATC instructions. Figure 1(a) provides an upper view of the described missed approach manoeuvre, assuming that air traffic controllers have provided clearance to proceed to TOLSU (the IAF)

Figure 1 Missed approach at Málaga RWY 13

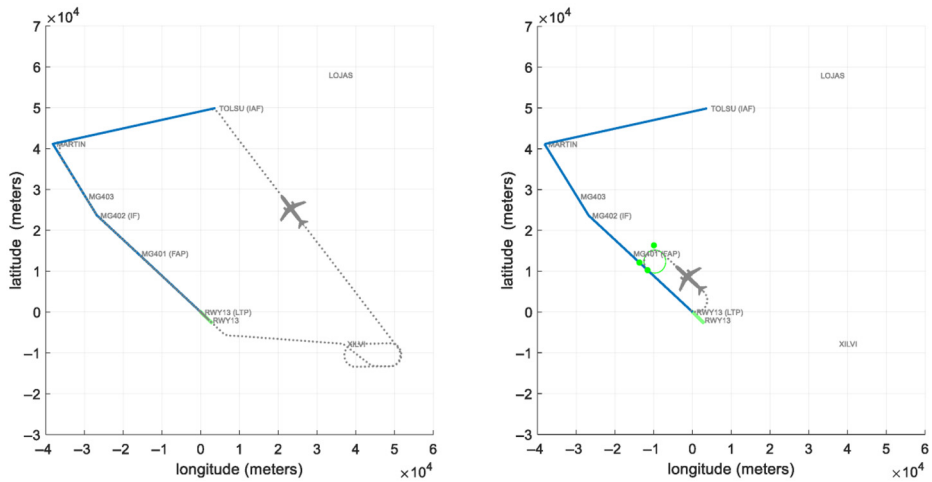

Notes: (a) Conventional procedure; (b) reinjection manoeuvre provided by ARS
Source: Figure by authors

once the aircraft has performed the holding pattern. The dotted line indicates the path followed by the aircraft after aborting the landing (at the MAPt).

The traditional missed approach manoeuvre described above introduces a high overhead to the total approach procedure. So, a previous work (Casado *et al.*, 2021) proposes an optimization from a theoretical and operational perspective. We now proceed to summarize such solution.

First, we assume that each approach is defined by a sequence of waypoints to be covered by aircraft. By default, it is provided by the chart, but we assume that air traffic controllers can modify, add and remove waypoints when necessary. We also assume that the ATC has up-to-date information on the airspace situation.

The proposed reinjection procedure is initiated when the pilot of an approaching aircraft notifies the ATC of his/her decision to execute a missed approach. The system must first determine the feasibility of executing a reinjection manoeuvre. This is accomplished by studying the approach flow in search of a gap between two consecutive aircraft that is large enough to allow the reinjection. The condition to be met is that the time difference between these two consecutive aircraft is greater than twice the aircraft spacing (T_s). Additionally, the gap must be located before a threshold time $T_1 \in T$ before the aircraft missing the approach.

If the search process finds a gap satisfying the above conditions, the algorithm assumes the existence of a "ghost" aircraft in the position corresponding to the minimum allowable time behind the aircraft associated to this gap. This ghost aircraft behaves the same as any other aircraft executing the approach manoeuvre. From this point, the ARS estimates the future position of the ghost aircraft and determines an intercepting trajectory for the aircraft missing the approach, so that both aircraft will meet at the reinjection point. This trajectory consists of three new auxiliary waypoints that the ATC must provide to the aircraft being reinjected.

Figure 1(b) shows the trajectory (dotted line) of an aircraft following a missed approach manoeuvre according to ARS in Málaga airport. For simplicity, we do not show the approach flow. Green dots indicate the auxiliary waypoints provided by ARS to guide the aircraft to the reinjection point. More details about ARS, including an implementation, can be found in (Casado *et al.*, 2021).

Base of Aircraft Data 3 model

BADA [European Organisation for the Safety of Air Navigation (Eurocontrol), 2023] provides a realistic model for determining the performance of any aircraft. Version 3 of its model family provides a coverage close to 100% of aircraft types, being considered a reference when attempting to achieve credible modelling of aircraft performances for the nominal part of the aircraft operational envelope.

For each aircraft analysed, BADA includes tables for climb, cruise and descent manoeuvres. For each manoeuvre and for certain altitudes, the table provides typical values of the behaviour of that aircraft (such as horizontal speed, vertical speed and instantaneous fuel consumption). Yet, neither a traditional missed approach manoeuvre nor a manoeuvre aimed at reinjecting the aircraft into the descent flow is comparable to a take-off situation, as the climb rate is much lower than for the latter. Consequently, in our study, it is not possible to apply the information in this database directly. Instead, we will use the underlying model through which these data were generated and which is described in this section.

Whenever the model requires data for a specific aircraft, we will choose the parameter values corresponding to the Airbus A320. Along with the Boeing 737, this aircraft model is the most popular passenger transport aircraft in recent decades. For this reason, it usually receives a great deal of attention in scientific works (Budd, 2012; Carvalho *et al.*, 2023; Cheung and Zhu, 2015; Dautermann *et al.*, 2018). Furthermore, according to the Spanish airport management company [*Aeropuertos Españoles y Navegación Aérea* (AENA), 2023], the total number of operations in the Málaga airport in 2022 was 144,123, out of 54,954 (that is, more than a third) were carried out by aircraft of the A320 family. The second most used aircraft family at this airport was the 737, with 45,476

operations (about 9500 less). Note that these two models account for more than two-thirds of the annual volume of operations at this airport. If we focus on arrivals, of the 72,071 operations in 2022, 27,478 (again, more than a third) were carried out by the A320.

Aircraft dynamics

To gain insight on the various factors affecting the aircraft dynamics, let us assume the situation shown in Figure 2. The aircraft moves in the direction and speed indicated by vector V, maintaining an angle of inclination γ with respect to the horizon. We will consider the stability coordinate system (stability axes), where the x axis is associated to the mentioned displacement and the y axis forms a right angle with the previous one. The movement of the aircraft generates an aerodynamic force that can be broken down into the vertical lift component L (which maintains the aircraft in the air), and the horizontal component of drag D (which acts as a friction force). BADA implements a simplified aerodynamic model in which it is assumed that the engines exert a propulsion force T in the direction of movement (thus maintaining a zero angle of attack). Finally, we denote the weight of the aircraft as $W = mg$.

The dynamic model could be decomposed in horizontal forces [equation (1)] and vertical forces [equation (2)]:

$$\sum F_x = T - D - Wsin\gamma \tag{1}$$

$$\sum F_y = L - Wcos\gamma \tag{2}$$

The advantage of the chosen reference system lies in the fact that the motion is exclusively in the horizontal axis. Applying Newton's second law to equation (3) and operating, we obtain what is known as the Total Energy Model:

$$\begin{gathered} m\dot{V} \wedge T - D - Wsin\gamma \\ mV\dot{V} \wedge VT - VD - WVsin\gamma \\ mV\dot{V} \wedge VT - VD - W\dot{h} \\ W\dot{h} + mV\dot{V} \wedge VT - VD \\ mg\dot{h} + mV\dot{V} \wedge VT - VD \\ mg\dot{h} + mV\dot{V} \wedge (T - D)V \end{gathered} \tag{3}$$

The two terms on the left side of the above expression correspond to the variation of potential and kinetic energy of the aircraft, respectively. The expression indicates that the energy variation is equal to force times velocity.

On the other hand, aerodynamic forces lift L and drag D are defined as:

$$L = C_L \frac{1}{2} \rho V^2 S \tag{4}$$

$$D = C_D \frac{1}{2} \rho V^2 S \tag{5}$$

The International Standard Atmosphere model [International Standard Organization (ISO), 1975] provides the air density at a certain geopotential height as $\rho = \frac{p}{RT_{air}}$. It is a function of the atmospheric pressure p, the air temperature T_{air} and a gas constant R that, for air, is equal to $287.05287\, m^2/(Ks^2)$. Additionally, according to BADA, an Airbus A320 aircraft has a wing area $S = 122.6\, m^2$.

Considering that there is no displacement in the vertical stability axis, by operating equation (2) and equation (4) we obtain $C_L \frac{1}{2} \rho V^2 S = mgcos\gamma$. Solving it, we can determine the lift coefficient as:

$$C_L = \frac{2mg}{\rho V^2 S} cos\gamma \tag{6}$$

Moreover, the drag coefficient is defined as:

$$C_D = C_{D_0} + C_{D_2} C_L^2 \tag{7}$$

where C_{D_0} and C_{D_2} are values that depend only on the level of deployment of flaps and gears.

These values are provided by BADA for the different flight modes. In our case, we have considered the CR (cruise), IC (initial climb) and AP (approaching) modes. By applying equation (6) and equation (7) in equation (5), we obtain the drag force.

Once the drag force D is obtained in equation (5), we can isolate the thrust T in equation (3), obtaining:

$$T = D + m\left(\frac{g\dot{h}}{V} + \dot{V}\right) \tag{8}$$

Fuel consumption

Based on the different equations presented above, we now proceed to derive the ones to determine the instantaneous fuel consumption. This will enable determining the overall fuel consumption associated to different manoeuvres.

BADA assumes two modes of fuel consumption called nominal and minimum. The nominal consumption model is applied in nearly all occasions. It is proportional to the propulsion force generated by the engines:

$$F_{nom} = \eta T \tag{9}$$

Such proportionality depends on the current speed (in knots), and on two constants C_{f1} and C_{f2} that BADA provides for each aircraft, as follows:

$$\eta = C_{f1}\left(1 + \frac{V}{C_{f2}}\right) \tag{10}$$

In case the aircraft is descending from a certain height (above 2,000 ft for the A320 aircraft), it is assumed that the pilot wants

Figure 2 BADA3 aircraft model

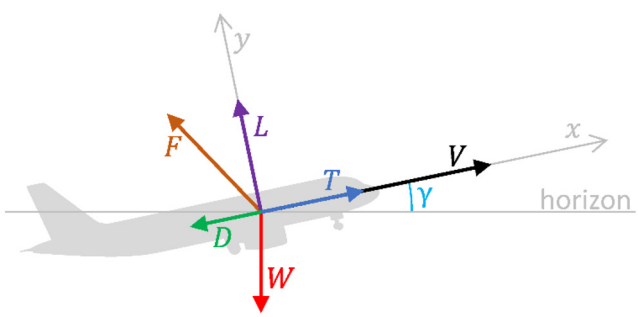

Source: Figure by authors

to reduce the horizontal speed, meaning that engines are in idle thrust mode. In this case, the minimum fuel consumption estimated by BADA depends on the geopotential height, and on other two constants C_{f3} and C_{f4}, as follows:

$$F_{min} = C_{f3}\left(1 - \frac{H_p}{C_{f4}}\right) \tag{11}$$

It is also worth mentioning that, in the troposphere (low altitude), the geopotential height H_p can be replaced (with negligible error) by the geometric height h provided by our simulator.

Algorithm 1 describes the instantaneous thrust calculation procedure. Initially, air density is obtained using a function implemented by MATLAB in its Aerospace blockset (Line 3). The lift coefficient is calculated according to equation (6) (Line 4). After that, we select the appropriate drag coefficients from BADA (Line 2) as a function of the current phase of the manoeuvre: ascending (Line 6), approaching (Line 8) or cruising (Line 10). With these coefficients, the drag coefficient is computed (Line 12) by applying equation (7). Then, the drag force is obtained (Line 13) applying equation (5). Finally, the engine thrust force (Line 14) is determined using equation (8).

Algorithm 1 Instantaneous Aircraft Thrust

1: procedure $InstantTrust(V, \dot{V}, \gamma, h, \dot{h})$
2: assume $C_{D_0IC}, C_{D_2IC}, C_{D_0AP}, C_{D_2AP}, C_{D_0CR}, C_{D_2CR}$
3: $\rho = atmosisa(h)$
4: $C_L = \frac{2mg}{\rho V^2 S} cos\gamma$
5: if $\dot{h} \geq 1$ then
6: $\{C_{D_0} C_{D_2}\} = \{C_{D_0IC} C_{D_2IC}\}$
7: elseif $\dot{h} \leq -1$
8: $\{C_{D_0} C_{D_2}\} = \{C_{D_0AP} C_{D_2AP}\}$
9: else
10: $\{C_{D_0} C_{D_2}\} = \{C_{D_0CR} C_{D_2CR}\}$
11: end if
12: $C_D = C_{D_0} + C_{D_2} C_L^2$
13: $D = C_D \frac{1}{2} \rho V^2 S$
14: $T = D + m\left(\frac{g\dot{h}}{V} + \dot{V}\right)$
15: return T
16: end procedure

Concerning Algorithm 2, it describes the instantaneous fuel consumption procedure. As stated before, there are two consumption models in BADA. The first one is the standard model. It assumes a fuel consumption (Line 7) proportional to the thrust force generated by the engines, according to equation (9). This proportionality (Line 6) depends on aircraft speed (Line 5) and on the two coefficients provided by BADA (Line 2) for this aircraft. The second consumption model (Line 9) uses equation (11) to compute idle engine consumption as a function of the aircraft altitude and the other two coefficients (Line 2) for this aircraft.

Algorithm 2 Instantaneous Aircraft Fuel Consumption

1: procedure $\boldsymbol{InstantFuel(\dot{h}, \dot{h}, T)}$
2: assume $\boldsymbol{C_{f1}, C_{f2}, C_{f3}, C_{f4}}$
3: $\boldsymbol{h_{ft} = feet(h)}$
4: if $\boldsymbol{\dot{h} \geq 0 \parallel h_{ft} < 2000}$ then
5: $\boldsymbol{V_{kt} = knots(V)}$
6: $\boldsymbol{\eta = \frac{C_{f1}}{1000}\left(1 + \frac{V_{kt}}{C_{f2}}\right)}$
7: $\boldsymbol{F = \eta T}$
8: else
9: $\boldsymbol{F = C_{f3}\left(1 - \frac{h_{ft}}{C_{f4}}\right)}$
10: end if
11: return $\boldsymbol{F}$
12: end procedure

Finally, Algorithm 3 describes the aggregated fuel consumption procedure over time. This algorithm executes an infinite loop (Line 3) in which it obtains the current aircraft dynamics parameters (Line 4) and computes instant engine thrust (Line 5) and fuel consumption (Line 6) (expressed in *Kg/min*). After that, it adds to the aggregated fuel value the portion corresponding to one second (Line 7). Then, this value is provided to external instruments (Line 8) that may require it. The whole procedure is repeated again after 1 s (Line 9).

Algorithm 3 Aggregated Aircraft Fuel Consumption

1: procedure $\boldsymbol{AggregateFuel}$
2: $\boldsymbol{F_a = 0}$
3: while $\boldsymbol{true}$ do
4: $\boldsymbol{get(V, \dot{V}, \gamma, h, \dot{h})}$
5: $\boldsymbol{T = InstantThrust(V, \dot{V}, \gamma, h, \dot{h})}$
6: $\boldsymbol{F = InstantFuel(\dot{h}, \dot{h}, T)}$
7: $\boldsymbol{F_a = F_a + \frac{F}{60}}$
8: $\boldsymbol{send(F_a)}$
9: $\boldsymbol{wait(1)}$
10: end while
11: end procedure

Methodology

The present study has been conducted by means of simulation. To assess the fuel consumption benefits of using the ARS instead of the conventional missed approach procedure, we have proceeded to incorporate the BADA model into our approach simulator. Next, we detail our simulation tool and how the different experiments were configured.

Our simulation model has been developed in MATLAB/Simulink R2022a (MathWorks, 2023), and considers the air traffic flow that approaches to a particular airport runway, including all the elements involved in an approach and landing manoeuvre. The tool combines time-based continuous and discrete-event simulation resources available in Simulink. It includes a configurable traffic generator that provides aircraft for the simulation. These aircraft appear in the airport airspace and proceed with the approach and landing procedures according to a programmed chart. We have considered the dynamics and the fuel consumption parameters for an Airbus A320 (see Section *BADA3 Model*). The ATC and the communications support that allow it to dynamically manage the sequences of waypoints followed by the aircraft have also been modelled.

For the experiments, the approach procedure for the RWY 13 runway at Málaga airport has been considered. It has been assumed that aircraft enter the airport airspace at LOJAS (at 7,000 ft), and they are immediately cleared to the IAF (TOLSU), without executing any holding pattern. Based on separation standards [International Civil Aviation Organization (ICAO), 2016], we have considered five different sequencing patterns, in which approaching aircraft are spaced by $T_s = 60\,s$, $T_s = 90\,s$, $T_s = 120\,s$, $T_s = 150\,s$ and $T_s = 180\,s$. We assume that air traffic controllers manage the aircraft sequence following a simple first-come first-serve strategy.

As stated, to reintroduce the aircraft into the descent flow when ARS is in place, a gap must be previously generated. For this, every certain number of aircraft, the ATC sequences the following aircraft after $2\,T_s$ seconds. Finally, it has been assumed $T_1 = 240\,s$, that is, with ARS an aircraft cannot be reinjected into a gap located less than 4 *min* away (see Section *Improving the Missed Approach Procedure*).

Simulation results

In this section we present the results of our study. Initially we assess the instantaneous fuel consumption for a missed approach

situation by comparing the results when an aircraft follows a conventional manoeuvre versus adopting the ARS reinjection procedure. The aircraft spacing is $T_s = 90\,s$. In the case of ARS, there are four aircraft between the one being reinjected and the gap. Figure 3 illustrates the results obtained. Figure 3 should be analysed in conjunction with Figure 1 to enhance comprehension of the trajectory followed by the aircraft in each case. Figure 3 comprises five plots, all sharing the horizontal axis, which represents time of flight. In each graph, scales in both the international (left) and aeronautical (right) systems have been incorporated for accurate representation. The red series represents the conventional re-injection mechanism, whereas the blue series depicts our ARS proposal.

The first plot in Figure 3 shows the aircraft's altitude profile. The graph displays the aircraft passage through various waypoints. Notably, disparities between the series start to appear when the aircraft reaches the MAPt. At this juncture, a noticeable altitude increase is observed, particularly pronounced in the conventional procedure. From this point onward, we can discern the transition to XILVI and a subsequent altitude increase to again execute the final approach from TOLSU. In the case of ARS, a smoother altitude increase occurs until reaching the designated reinjection point, followed by a final descend to the runway. The second plot shows vertical speed and corresponds to the derivative of the first plot. The vertical speed is adjusted to ensure that the aircraft reaches the altitude specified at the

Figure 3 Instantaneous comparison between the conventional missed approach procedure and ARS

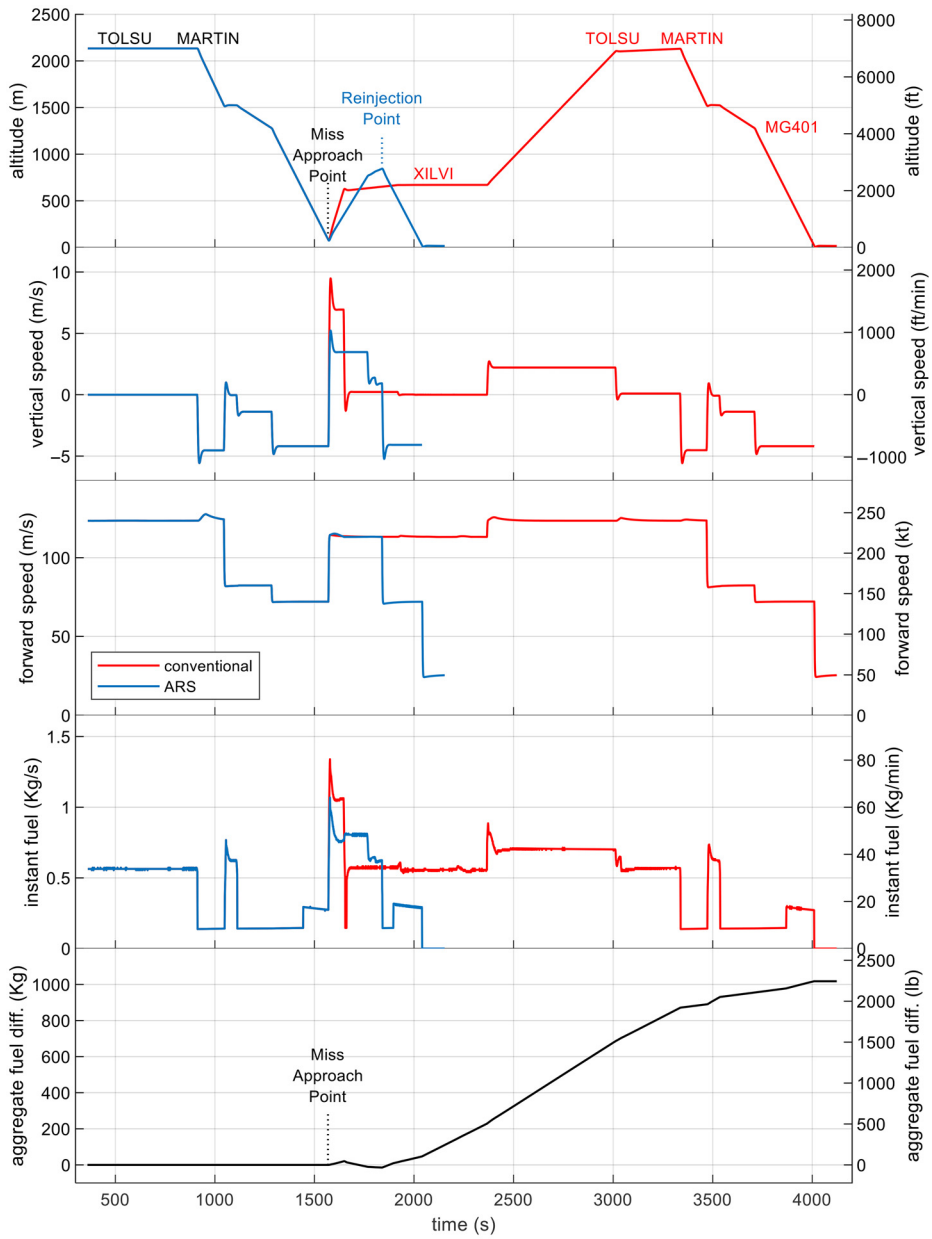

Source: Figure by authors

waypoint precisely when it reaches the waypoint in the horizontal plane. The third plot displays forward speed. It is evident that, as the aircraft transitions to a new waypoint, it adjusts its velocity to match the indicated speed, maintaining it constant throughout the entire segment.

The fourth plot in Figure 3 illustrates instant fuel consumption. As anticipated, it showcases a similar behaviour to was presented in the second plot. In both plots, a peak is evident, aligning with the abrupt ascent of the aircraft after the MAPt. In the case of the conventional procedure, this peak in speed and fuel consumption is more pronounced because, despite the aircraft is climbing up to a lower altitude, it does so in a shorter timeframe. The last plot in Figure 3 displays the difference in fuel consumed aggregated over time. As expected, significant disparities between the two approaches manifest after the moment when the aircraft following the ARS procedure lands. At this point, fuel consumption becomes negligible for the ARS-enabled aircraft, while flight operations persist for a substantial duration for aircraft using the conventional procedure. Consequently, in this scenario, landing with ARS translates to a fuel saving of about 1,000 *kg*.

Figure 4(a) displays the time savings achieved with the implementation of ARS at Málaga airport, using the time required for the conventional missed approach procedure as the reference. To derive these results, in each simulation experiment, we measured the time elapsed between the two times the aircraft reaches the MAPt: the moment it decides to abort the landing and when it completes the manoeuvre. The series indicate sequencing patterns (ranging from 1 to 3 *min*). The horizontal axis represents the number of aircraft in the approach flow between the one initiating the missed approach and the reinjection gap. Higher values for both these parameters naturally imply greater distances to the gap, resulting in longer flight times and consequently diminishing the effectiveness of ARS. Nevertheless, across all scenarios, time savings are evident, albeit diminishing as the distance to the gap increases, yet consistently remaining above 50%.

Fuel consumption savings in the aforementioned configurations were also examined using the model outlined in Section *Fuel Consumption*. Figure 4(b) showcases the outcomes. Once again, the results are normalized relative to the fuel consumed during the conventional missed approach procedure. As anticipated, the observed time savings directly correlate with fuel savings.

To complete the present study, we have repeated the experiment that gave rise to the results shown in Figure 3, but customizing our simulation tool with the specific parameters of the other two major aircraft models operating at Málaga airport, which are the Boeing 737 and the ATR 72 [*Aeropuertos Españoles y Navegación Aérea* (AENA), 2023]. The Boeing 737 is a narrow-body aircraft, comparable in performance to the A320. On the other hand, the ATR 72 is a regional aircraft. To cover other aircraft segments, we have also incorporated to this final experiment the Boeing 777, a large wide-body aircraft. The results presented in Table 1 indicate that in all cases ARS consumes about 20% of the fuel consumed by a conventional missed approach procedure. In other words, as in the case of the A320, we are moving in fuel savings of 80%.

Discussion

The mechanism described in the study has several potential implications for society, including commercial and economic aspects. The first of these would be that, by enhancing the efficiency of the approach and landing procedures, the ARS system has a direct impact on flight punctuality and passenger comfort, thus enhancing the travel experience and reducing delays.

On the other hand, as fuel economy becomes a more critical factor in flight operations, approaches such as the one proposed in this paper emerge as a solution to partially mitigate such challenge by reducing the high fuel wastage associated to missed approaches at airports (Murrieta-Mendoza and Botez, 2016). Yet, each airport, based on saturation indexes, aircraft spacing and other factors, should devise when to introduce reinjection gaps, i.e. the frequency at which such gaps should take place, as their presence is a requirement for ARS solutions to be adopted. In fact, since introducing gaps might have a slightly negative

Table 1 Total fuel consumption during the approach procedure and relative consumption for different aircraft models

Aircraft model	Conventional (kg)	ARS (kg)	Conv./ARS (%)
Airbus A320	1,274.8	257.1	20.17
Boeing 737	1,267.8	265.2	20.92
ATR 72	1,791.0	330.7	18.46
Boeing 777	4,699.6	977.5	20.80

Source: Table by authors

Figure 4 Normalized time and fuel savings as a function of the distance to the gap

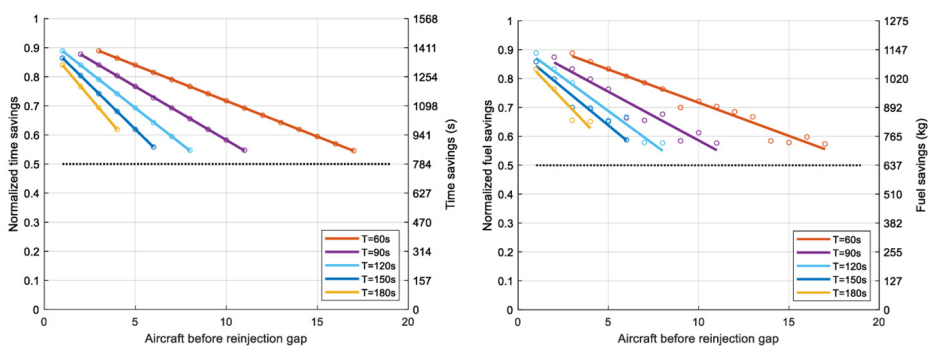

(a) (b)

Source: Figure by authors

impact on the flight time/fuel consumption of the different incoming aircraft, the operation experts at each airport should study the frequency of missed approaches, the typical landing frequency and other relevant parameters such as type of aircraft, to determine the most adequate gap insertion criteria for that particular airport. In this direction, the details presented in this paper can clearly guide such process by highlighting the key parameters and expected time/fuel savings under different conditions; such savings must be fine-tuned considering the characteristics of each airport to have a more detailed and realistic assessment following our proposed approach.

Conclusions

From the three phases of a flight (take-off, cruise and landing), it seems that those which imply significant vertical displacements still offer optimizations regarding fuel savings from the aircraft operation point of view. Take-off and landing phases are associated to important engine demands, and these manoeuvres are conditioned by severe safety restrictions. Also, these manoeuvres take place close to airports, affecting populated areas.

In a previous work, a new procedure to be used in case of missed approaches was proposed. An analytical model for this new method was developed, and it was validated through simulation techniques. In this paper we have extended such model to provide an estimation of the fuel savings which could be obtained with the new ARS procedure. We prove that a least a 50% of fuel savings is obtained when compared with the traditional method. Obviously, these savings would be related with a reduction of CO_2 and other pollutants.

Future work

Continuing with this promising research work, and given the immediate benefits it could provide, we will extend the study to evaluate the impact on noise and pollution. Also, a model of the *ghost* slots required by the ARS method should be developed to evaluate its impact on the whole airport performance.

References

Aeropuertos Españoles y Navegación Aérea (AENA) (2023), "Estadísticas de tráfico aereo", available at: www.aena.es/es/estadisticas/inicio.html (accessed 13 October 2023).

Boeing (2007), "Fuel conservation strategies", AERO Magazine, available at: www.boeing.com/commercial/aeromagazine/articles/qtr_2_07/article_05_1.html (accessed 8 October 2023).

Budd, L.C.S. (2012), "The potential use of consumer flight radar apps as a source of empirical data: a study of A320 utilization rates in Europe", *Journal of Air Transport Management*, Vol. 25, pp. 53-56, doi: 10.1016/j.jairtraman.2012.08.004.

Carvalho, H., Gomes, R.A. and Caetano, M. (2023), "Technological aircraft evolution and aviation emissions: an environmental progress case for the A320 family in Brazil", *International Journal of Environmental Science and Technology*, Vol. 21 No. 1, doi: 10.1007/s13762-023-04952-3.

Casado, R., Lopez-Lago, M., Serna, J. and Bermudez, A. (2021), "Enhanced missed approach procedure based on aircraft reinjection", *IEEE Transactions on Aerospace and Electronic Systems*, Vol. 57 No. 6, pp. 4149-4170, doi: 10.1109/TAES.2021.3082666.

Cheung, C.W. and Zhu, Q.M. (2015), "Modelling flight dynamics for the airbus A320", *2015 7th International Conference on Modelling, Identification and Control (ICMIC)*, pp. 1-7, doi: 10.1109/ICMIC.2015.7409340.

Dancila, R., Botez, R. and Ford, S. (2013), "Fuel burn and emissions evaluation for a missed approach procedure performed by a B737-400", *2013 Aviation Technology, Integration, and Operations Conference*, doi: 10.2514/6.2013-4387.

Dautermann, T., Altenscheidt, L., Ludwig, T., Altenscheidt, M. and Geister, R. (2018), "Performance comparison of A320 and 737ng regarding the vertical and speed Pro-Files in advanced RNP to XLS arrivals", *2018 IEEE/AIAA 37th Digital Avionics Systems Conference (DASC)*, pp. 1-5, doi: 10.1109/DASC.2018.8569819.

European Environment Agency (EEA) (2023), "EMEP/EEA air pollutant emission inventory guidebook", available at: www.eea.europa.eu/themes/air/air-pollution-sources-1/emep-eea-air-pollutant-emission-inventory-guidebook (accessed 8 October 2023).

European Organisation for the Safety of Air Navigation (Eurocontrol) (2023), "BADA: aircraft performance model", available at: www.eurocontrol.int/model/bada (accessed 8 October 2023).

European Union Aviation Safety Agency (EASA) (2019), "European aviation environmental report", available at: www.easa.europa.eu/eco/sites/default/files/2021-09/219473_EASA_EAER_2019_WEB_HI-RES_190311.pdf (accessed 8 October 2023).

Federal Aviation Administration (FAA) (2023a), "Instrument procedures handbook (IPH)", available at: www.faa.gov/regulations_policies/handbooks_manuals/aviation/instrument_procedures_handbook/ (accessed 8 October 2023).

Federal Aviation Administration (FAA) (2023b), "Aeronautical information manual (AIM)", available at: www.faa.gov/air_traffic/publications/atpubs/aim_html/ (accessed 8 October 2023).

Harada, A., Miyamoto, Y., Miyazawa, Y. and Funabiki, K. (2013), "Accuracy evaluation of an aircraft performance model with airliner flight data", *Transactions of the Japan Society for Aeronautical and Space Sciences, Aerospace Technology Japan*, Vol. 11 No. 0, pp. 79-85, doi: 10.2322/tastj.11.79.

International Civil Aviation Organization (ICAO) (2016), *Doc 4444 – PANS-ATM, Procedures for Air Navigation Services – Air Traffic Management*, edited by ICAO, 16th ed., Montreal.

International Civil Aviation Organization (ICAO) (2023), "Málaga/costa del sol GBAS Z RWY 13 instrument approach chart", available at: www.aip.enaire.es/aip/contenido_AIP/AD/AD2/LEMG/LE_AD_2_LEMG_IAC_11_en.pdf (accessed 8 October 2023).

International Standard Organization (ISO) (1975), "ISO 2533:1975 standard atmosphere", available at: www.iso.org/standard/7472.html (accessed 8 October 2023).

Lu, C. and Morrell, P. (2006), "Determination and applications of environmental costs at different sized airports–aircraft noise and engine emissions", *Transportation, Springer*, Vol. 33 No. 1, pp. 45-61.

MathWorks (2023), "Matlab", available at: www.mathworks.com/products/matlab.html (accessed 8 October 2023).

Moir, I., Seabridge, A. and Jukes, M. (2013), *Civil Avionics Systems, Civil Avionics Systems*, Wiley, doi: 10.1002/9781118536704.

Murrieta-Mendoza, A. and Botez, R.M. (2016), "New method to compute the missed approach fuel consumption and its emissions", *The Aeronautical Journal*, Vol. 120 No. 1228, pp. 910-929, doi: 10.1017/aer.2016.37.

Nuic, A., Poles, D. and Mouillet, V. (2010), "BADA: an advanced aircraft performance model for present and future ATM systems", *International Journal of Adaptive Control and Signal Processing*, Vol. 24 No. 10, pp. 850-866, doi: 10.1002/acs.1176.

Poles, D., Nuic, A. and Mouillet, V. (2010), "Advanced aircraft performance modeling for ATM: analysis of BADA model capabilities", *29th Digital Avionics Systems Conference*, IEEE, pp. 1.D.1-1-1.D.1-14, doi: 10.1109/DASC.2010.5655518.

Corresponding author

Rafael Casado González can be contacted at: Rafael.Casado@uclm.es